Inorganica Chimica Acta 565 (2024) 122000

Contents lists available at ScienceDirect

Inorganica Chimica Acta

journal homepage: www.elsevier.com/locate/ica

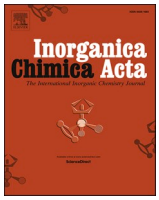

Supramolecular self-assembly dicopper carboxylates metallogels driven by non-covalent interactions and pi-pi stacking: Crystal structure and bioinspired catalysis

Sunshine Dominic Kurbah [a,*], Ndege Simisi Clovis [b]

[a] Department of Chemistry, Pandit Deendayal Upadhyaya Adarsha Mahavidyalaya, Eraligool-788723, Karimganj, Assam, India
[b] Department of Chemistry, Faculty of Science and Technology, University of Kinshasa, Kinshasa, Democratic Republic of Congo

ARTICLE INFO

Keywords:
Bimetallic
Metallogel
Copper
Supramolecular
Bioinspired
Catalyst

ABSTRACT

A new bimetallic metallogel was synthesized and characterized by various spectroscopic techniques. The morphology of BMG has been explained with the help of scanning electron microscopy. The rheological investigation helps to examine the supramolecular BMG metallogel. It was found that the G′ value was significantly larger compare to G″ value, which confirmed the gel nature of the material. Single X-ray diffraction studies verified the existence of pi-pi stacking, non-covalent interactions, and other short molecule interactions necessary for the formation of metallogel. Furthermore, copper-based metallogel BMG can be utilized as a catalyst for aerobic oxidation of 3,5-di-*tert*-butylcatechol (3,5-DTBC) to 3,5-di-*tert*-butyl benzoquinone (3,5-DTBQ). The kinetic parameters were obtained by plotting rate vs. substrate concentration of BMG based on Michaelis–Menten approach of enzymatic kinetics. To the best of our knowledge, only few metallogel materials were reported for bioinspired catalysis like catechol oxidation.

1. Introduction

In recent years, supramolecular gels with stimuli-responsive properties have become one of the most significant realms and attracted increasing attention because of their promising applications in the field of biomaterials, catalysis, drug delivery, sensors, chemical engineering, optoelectronics, displays and other relevant areas [1–6]. In this regard, although many organic low molecular weight gelators have been reported but metal containing systems have only more recently begun to receive significant attention [7,8]. The incorporation of metal ions to control molecular assembly is also a well-recognized strategy for constructing gels, in which the facile and dynamic metal–ligand coordination interaction endows the gel with unique and new properties that permits the design of many materials that enhanced catalytic performance [9,10], conductivity [11], luminescence [12], magnetism [13], redox behaviour [14], electronic devices [15], as well as selective and sensitive sensing that are difficult to achieve by organic systems [16].

Typically, up to date many metallogels have been created using metal complexes containing organic gelators [17,18]. The incorporation of metal ions into gels brings new properties to the system. Supramolecular metallogels having stimuli-responsive abilities can be constructed, taking advantage of the dynamic and reversible nature of weak forces formed through non-covalent intermolecular interactions, such as π-π stacking, hydrogen bonding and electrostatic interactions [19,20]. These excellent properties would bring benefit to the applications of smart materials. Remarkably, the metallogels are less explored in comparison to organic gels because of difficulty in synthesis, characterization as well as prediction of mechanism behind gelation [21,22]. To the best of our efforts, we have successfully achieved in synthesizing bimetallic copper metallogels constructed from simple carboxylate and 2,2′ bipyridine ligands. The synthetic metallogel was used as a bioinspired catalyst for efficient oxidation of catechol to *o*-benzoquinone.

2. Experimental

2.1. Physical measurements

Solvents were reagent grade and used as received. Other chemicals such as benzoic acid, 2, 2′-bipyridine, Ammonium hexafluorophosphate were purchased from Sigma Aldrich and were used as received without any further purification. Copper acetate, and other metal salts were purchased from HiMedia and were used as received. All operations were

* Corresponding author.
E-mail address: sunshinekurbah@yahoo.com (S. Dominic Kurbah).

https://doi.org/10.1016/j.ica.2024.122000
Received 26 October 2023; Received in revised form 26 January 2024; Accepted 27 February 2024
Available online 28 February 2024

performed under aerobic conditions. Infrared spectra in the range 4000–200 cm^{-1} were recorded as KBr discs by using a BX-III/ FTIR Perkin Elmer Spectrophotometer. Solution electronic spectra were recorded on a Perkin-Elmer Lambda-25 spectrophotometer.

2.2. Single crystal X-ray crystallography

Single crystal X-ray data were collected at 291.8 K, using an Xcalibur, Eos, Gemini diffractometer equipped with monochromated Mo K radiation (l = 0.71073 A). The CrysAlis PRO, Agilent, 2013 software package was used for data collection and reduction. The intensity data were corrected using a semi empirical absorption method. In all cases absorption corrections based on multiscan using SADABS software were applied. The crystal structure was solved and refined using SHELXL-2014 [32,33]. All non-hydrogen atoms were refined anisotropically, whereas the hydrogen atoms were place at a calculated position and refined in the final refinement.

Crystallographic data of BMG have been deposited with the Cambridge Crystallographic Data Centre, CCDC, 12 Union Road, Cambridge CB21EZ, UK. Copies of the data can be obtained free of charge on quoting the depository number CCDC-2310383 (deposit@ccdc.cam.ac.uk, https://www.ccdc.cam.ac.uk).

2.3. Preparation of metallogel (BMG)

In a typical gel formation reaction, a mixtures of $Cu(OAc)_2{\cdot}H_2O$ (0.10 g, 0.5 mmol), benzoic acid (0.061 g, 0.5 mmol), 2, 2‘ bipyridine (0.075 g, 0.5 mmol) and NH_4PF_6 (0.08 g, 0.5 mmol) was dissolved in DMF/water 5 mL (v/v 1:4) in a vial and stirred for 20 min to get a clear blue solution. The mixture was kept undisturbed until the gel formation occurred for few minutes. Then, the formation of gel was confirmed by the glass vial inversion method at room temperature (Scheme S1). Single crystal of metallogels was obtained by slow evaporation of BMG at room temperature for 6 days. Color: dark blue. IR data (cm^{-1}, KBr): 1599 s, 1567 s (v_{as} COO), 1446 s, 1384 s v_s (COO); 729 s, 678 s, 1022–1033 ν (PF_6^-). Electronic spectrum: CH_3CN solution, λ_{max} (nm): 678 nm. Diffraction quality crystals of BMG were obtained by slow evaporation of reaction mixture at room temperature. Yield: 87 %. Melting point: 247 °C.

2.4. Scanning electron microscopy (SEM)

The morphology of the synthesized BMG metallogel was characterized using a scanning electron microscope (JSM-6360, Jeol, with an Oxford EDS detector) operating at 1–30 kV. For sample preparation, a diluted sample of the metallogel was put onto a thin aluminum sheet by using a capillary tube and then allowed to dry in air. The sample was also coated with a thin layer of Au before the experiment to minimize sample charging.

3. Results and discussion

3.1. Synthesis and characterization

Coordination compound typically produces metallogels in the right solvents, although precise gelation prediction in an organic solvent remains difficult. Many studies have shown that the formation of the metallogels requires a cross-linked, three-dimensional network, created by a correct combination of ligands and transition-metal ions with many coordination sites. In our study we began by treating ligand with metal (1:1:1 M ratio) using different solvents combination. The gelation experiments were carried out using “stable to inversion of a test tube” method in various solvents such as water, methanol, chloroform, toluene, DMSO, water/methanol. Thus, after several attempts it was observed that gelation formed in mixed DMF/water (1:3 to 1:9 (v/v)) (Scheme 1). The metallogel exhibits excellent gelation abilities and turned out to be quite efficient, displaying a 1.4 wt% minimum gelator concentration with a gel-sol dissociation temperature, T_{gel}, of 62 °C (DMF/water) measured by using the ‘tilted tube’ method (Scheme S1). The gel was stable on standing at room temperature for several weeks and for months when stored below 10 °C, with only a slight darkening of colour. The sol undergoes re-gelation when sonicated followed by heating at 75 °C. The gel can also be synthesized in bulk scale in a similar manner. The metallogel is soluble in methanol, ethanol, acetonitrile, dimethylsulfoxide (DMSO) and dimethylformamide (DMF).

Absorption spectrum of the gel was recorded at room temperature in acetonitrile solution. A broad absorption band at 678 nm was observed, this band arises due to d-d transition. In order to understand the gelation process and participation of ligands in bonding toward metal ions, Fourier transform infrared (FT-IR) spectroscopy of the gels was recorded (Figure S1). The IR spectra of BMG shows peak at 729 cm^{-1} was assigned to in- plane stretching vibrations of 2,2-bipyridine ligand and whereas the peak at 678 cm^{-1} was assigned to out- of- plane ring deformation mode of 2,2′-bipyridine ligand. The asymmetric carboxylate COO^- stretching vibrations of the benzoate ligands are in the region of 1600–1567 cm^{-1} whereas symmetric carboxylate COO^- stretching vibrations appear in the range of 1383–1447 cm^{-1} and PF_6^- ions bands appeared at 1022 and 1033 cm^{-1}, respectively.

3.2. Gelation studies

During the metallogel formation, various interactions contained in the structural units and crystal lattice of BMG, including non-covalent interactions and pi-pi stacking interactions between aromatic rings,

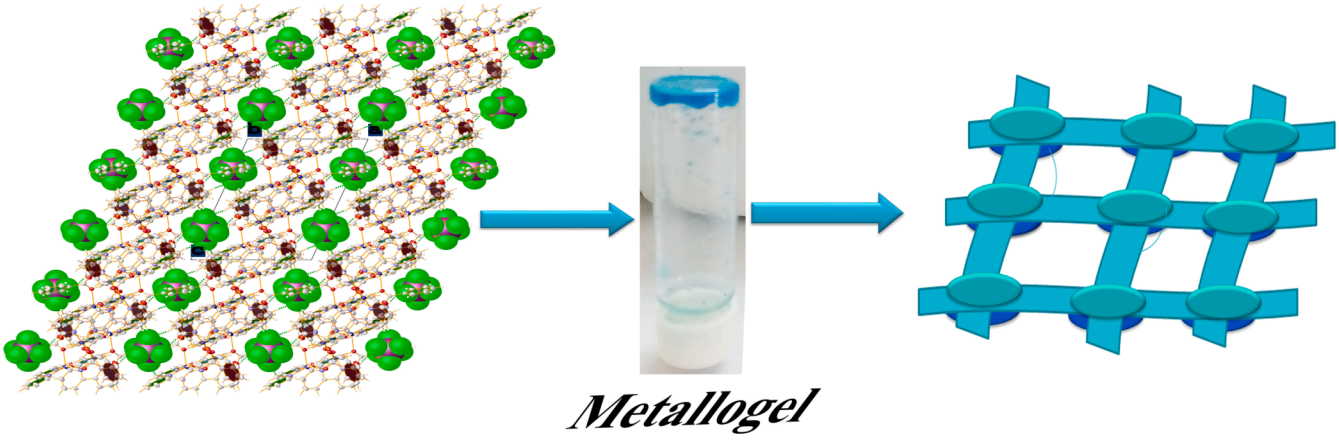

Scheme 1. Schematic Presentation of Formation of Metallogel.

may have played significant roles and worked in concert to stabilize the gel structure during the metallogel formation. We have recorded the SEM images of the gels in order to gain an insight into the microstructure of the gels formed due to a solvent mediated self-assembly process. The SEM image of BMG shows that material exists as agglomerates of very fine particles and even the size of the agglomerates appears to be much less than 5 μm (Fig. 1). The physical characteristics of the gel demonstrate that the substance occurs as aggregates of extremely small particles. These smaller particles prefer to stay in the most thermodynamically advantageous condition because they are packed into larger particles with pores in between. These smaller particles combine to make bigger particles, which then combine to form a typical supramolecular structure. Particles agglomerations may be due to the interaction between the solvent and the gels, which happened due to relatively large van der Waals forces of attraction and other short interaction presence inside the metallogels. The rheological investigation helps to examine the supramolecular BMG metallogel's mechanical characteristics. The viscous and elastic characteristics of gel materials are demonstrated by the results of rheological testing and and the metallogel strength is characterized by storage (G′) and loss modulus (G″), respectively. The dynamic frequency sweep experiment is shown in Figure S2. Here, we discover a broad region of linear viscoelasticity where G′ and G″ are almost independent of frequency variations. It was found that the G′ value was significantly larger compare to G″ value, confirming the gel nature of the material (BMG).

Additionally, single X-ray diffraction studies verified the existence of pi-pi stacking, non-covalent interactions, and other short molecule interactions necessary for the formation of metallogel. The BMG is made up of weak inter and intra molecule hydrogen bonding interactions such C—H··F, C—H..O, and C—H··F (Fig. 2). The C—H··F interaction bond distances are 3.135(8) Å (C3-H3··F1) and 3.237(10) Å (C20-H20··F5), whereas the C—H··O interaction are 2.958(6) Å (C10-*H*10··O3), 3.015 (5) Å (C20-H20··O5) and 3.015(5) Å (C20-H20··O5). The intermolecular interactions are further described by the 2D fingerprint plots. The major contributors to the crystal packing are interactions H···H (39 %), followed by H···C/ H···C (27 %), H···C/ H···C (14 %), and H···O/ O···H (10 %), whereas other remaining contact are negligible (Fig. 3). In this study, two-dimensional hydrogen-bonded assemblies with fascinating supramolecular frameworks were created via hydrogen bonding and non-covalent interactions.

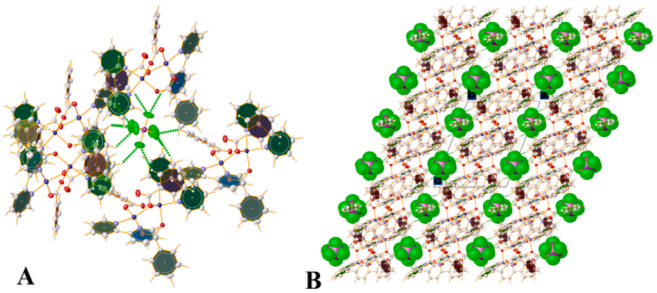

Fig. 2. (A) Packing diagram of BMG along crystallographic b-axis, (B) Molecular interactions presence in the crystal structure.

3.3. Crystal structure of BMG

Crystal structure of was obtained by reacting the appropriate ligands and the metal salts in a solvent environment similar to that employed for gelation, we attempted to obtain the thermodynamically more stable neat single crystals of the gelling agents. Single crystal of BMG suitable for single crystal x-ray analysis were obtained from methanol solution at room temperature for six days, BMG crystallized in monoclinic with $P2_1/c$ space group. Molecular structure of BMG is shown in Fig. 4, crystal data and structure refinement of the are given in Table.1, whereas selected bond lengths and bond angles are given in Table S1 and S2. The molecular structure of BMG consists of two copper(II) center, two bipyridine ligand on each side of metal ions, three benzoic acids ligands which bind toward the metal center both in mono and bi-dentate bridging fashion. The metal ions exhibit a MN_2O_3 coordination environment. The metal bond distances around Cu1 are 1.983(3) Å (Cu1-O1), 1.923(3) Å (Cu1-O3), 2.192(3) Å (Cu1-O5), 2.001(3) Å (Cu1-N1), 1.999(3) Å (Cu1-N2), whereas the metal bond distances around Cu2 are 1.961(3) Å (Cu2-O2), 2.170(3) Å (Cu2-O4), 1.967(2) Å (Cu2-O5), 2.022 (3) Å (Cu2-N3) and 2.001(3) Å (Cu2-N4). The geometrical bond angles of BMG are 92.19(11)° (O3-Cu1-O5), 95.38(11)° (O3-Cu1-O1), 91.39 (12)° (O3-Cu1-N2), 171.90(11)° (O3-Cu1-N1), 97.23(10)° (O1-Cu1-O5), 142.65(12)° (O1-Cu1-N2), 91.94(11)° (O1-Cu1-N1), 119.20(11)° (N2-Cu1-O5), 80.66(12)° (N2-Cu1-N1), 90.34(11)° (N1-Cu1-O5), 96.46 (11)° (O2-Cu2-O5), 95.13(11)° (O2-Cu2-O4), 91.75(12)° (O2-Cu2-N3), 171.70(11)° (O2-Cu2-N4), 96.71(10)° (O5-Cu2-O4), 151.56(12)° (O5-Cu2-N3), 90.54(11)° (O5-Cu2-N4), 109.65(11)° (N3-Cu2-O4), 88.45 (12)° (N4-Cu2-O4) and 79.98(13)° (N4-Cu2-N3). The trans angles in BMG are, with geometrical index, $\tau_5 = 0.49$ in Cu1; whereas in Cu2, the

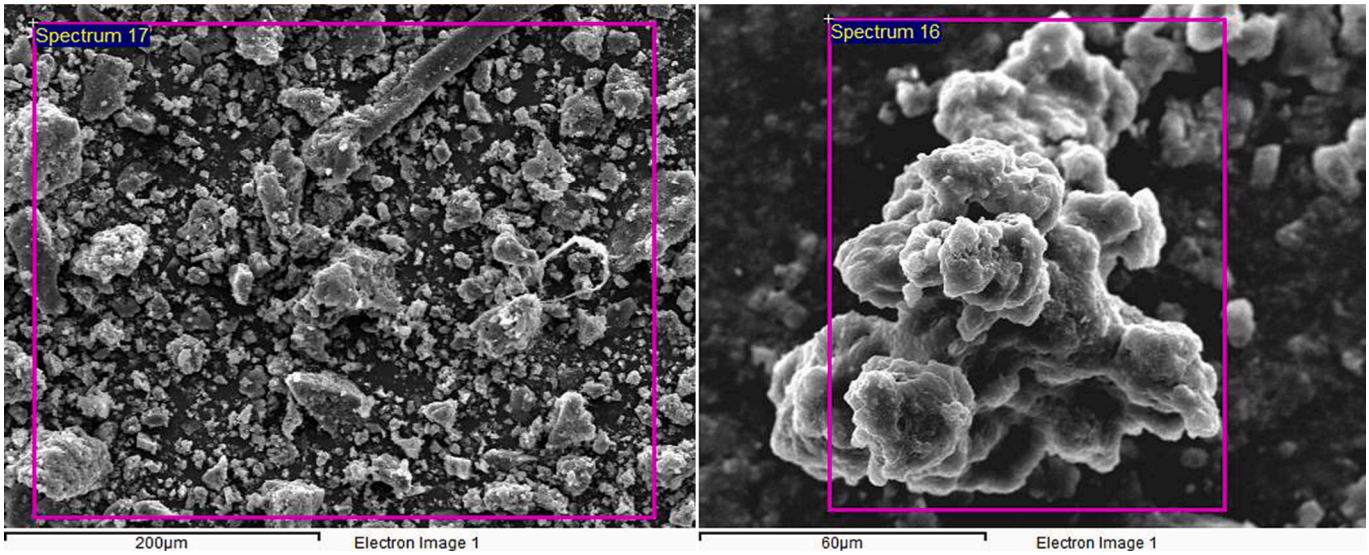

Fig. 1. SEM image of the metallogels.

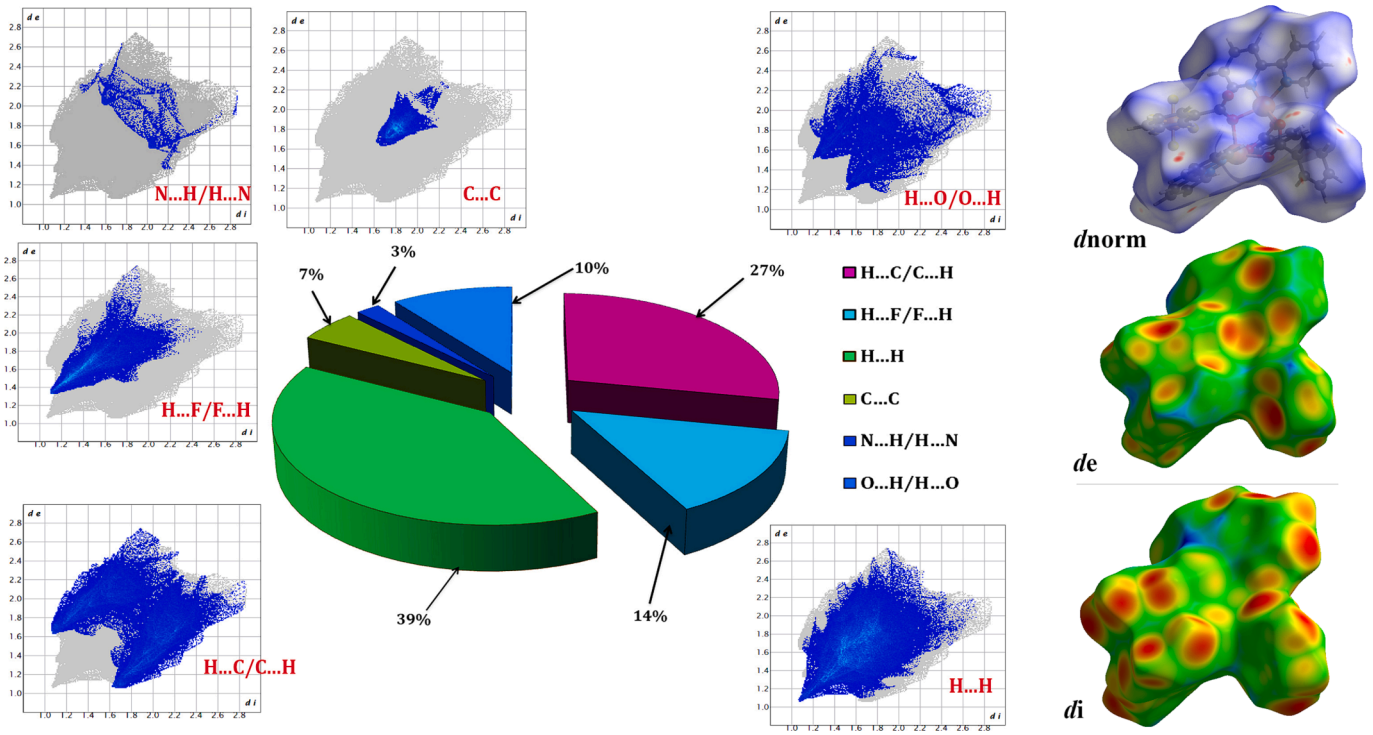

Fig. 3. Fingerprint plots, pi-chart representing the overall contribution and hirshfeld surface plot for (i) dnorm (ii) de and (iii) di.

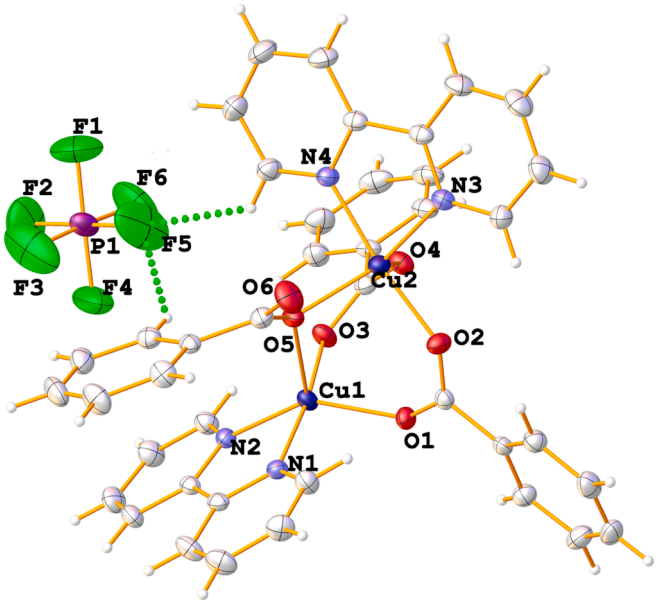

Fig. 4. ORTEP diagram of BMG metallogel (Color of atoms: Carbon atom are highlighted in gray white, Fluorine in green, Phosphorus in purple, Nitrogen in navy blue, Oxygen in red and hydrogen in Gray white, solid bond between atoms are highlighted in orange, hydrogen bonding between fluorine and hydrogen in green color).

trans angles are with $\tau_5 = 0.34$. The indexing parameters suggested that both the copper(II) centers adopted a square pyramidal geometry with slight distortion.

3.4. Catechol oxidase like activity of BMG

Catechol oxidase is a type-III dinuclear copper(II) enzyme that catalyses the oxidation of catechol to the corresponding o-quinone while reducing molecular oxygen to water molecules [23]. The met form of the enzyme's crystal structure revealed that the active site consists of a dicopper(II) center bridged by a hydroxo group, three histidine nitrogen coordinated to each copper(II) center, and one nitrogen at the apical site, forming a trigonal pyramidal geometry [24,25]. To replicate the enzyme active site, many dicopper(II) complexes containing comparable ligands were developed [26–28]. In our study we investigated the catechol oxidase like activity of BMG as a pre-catalyst and using 3,5-di-*tert*-butylcatechol (3,5-DTBC) as a substrate under aerobic conditions at room temperature. The reaction was initiated by reacting 1.2×10^{-4} M solution of metallogel with an increasing amount of 3,5-di-*tert*-butylcatechol from 1×10^{-3} to 1.5×10^{-2} M in DMSO in the presence of air. The formation of the products was spectrophotometrically monitored by measuring the absorption band at 402 nm, which is the characteristic absorption band of 3,5-di-*tert*-butylquinone (3,5-DTBQ) as shown in

Table 1
Crystal data and structure refinement BMG.

Empirical formula	$C_{41}H_{31}N_4O_6F_6PCu_2$
Formula weight	947.75
Temperature/K	291.9(5)
Crystal system	monoclinic
Space group	*P*21/*c*
a/Å	11.5450(7)
b/Å	22.2157(7)
c/Å	15.9234(7)
α/°	90
β/°	109.870(6)
γ/°	90
Volume/Å3	3840.9(3)
Z	4
Radiation	Mo Kα (λ = 0.71073)
Reflections collected	16,786
Data/restraints/parameters	6758/0/541
Goodness-of-fit on F2	1.028
Final R indexes [I>=2σ (I)]	R1 = 0.0455, w*R*2 = 0.1155
Final R indexes [all data]	R1 = 0.0671, w*R*2 = 0.1277
Largest diff. peak/hole / e Å^{-3}	0.77/-0.39

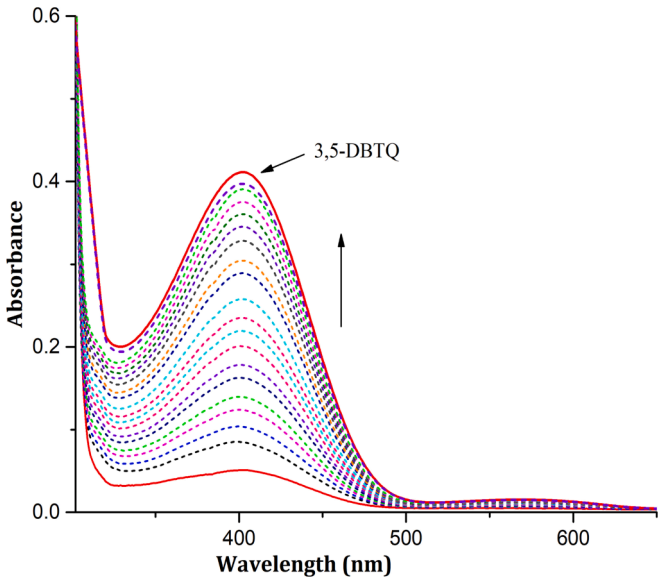

Fig. 5a. (A) Spectral changes observed for the absorbance at 402 nm as function of time (recorded at 2 min intervals).

Fig. 5. The peak at 402 nm became more intense with the time, which indicated that the BMG metallogel can act as an efficient catalyst for oxidation of 3,5-DTBC to 3,5-DTBQ. To test the versatility of the newly synthesized BMG, we carried out the catalytic oxidation of other substrates by using tetrachlorocatechol (TTC). The catalytic oxidation of tetrachlorocatechol (TTC) to tetrachloroquinone (TTQ) was carried out successfully, and the formation of the products was monitored spectrophotometrically by measuring the absorption band at 415 nm, which is the characteristic absorption band of TTQ [38]. As shown in Fig. 6, the conversion of tetrachlorocatechol (TTC) to tetrachloroquinone (TTQ) does not take place in the absence of BMG. But with the addition of BMG, the intensity of tetrachloroquinone increases with time. Hence, the BMG metallogel acts as a catalyst to speed up the catalytic process for the oxidation of tetrachlorocatechol to tetrachloroquinone. Therefore, in our attempt, we have successfully synthesized similar copper(II) model complexes for catechol oxidase activity to disseminate the mechanism and generate efficient mimics.

To understand the kinetic feature of catalysis for BMG metallogel, the rate constant for the catalytic reaction was calculated using the initial rate method. Next, the observed rate versus substrate concentration data was analysed using the Michaelis-Menten method of enzymatic kinetics [29]. Observed rate vs. substrate concentration data are then examined based on Michaelis–Menten approach of enzymatic kinetics in order to calculate values of V_{max}, K_M and K_{cat}. From the plot, the kinetics parameters, KM = 1.98×10^{-3} M (Michaelis constant), V_{max} = 4.3×10^{-2} M min^{-1} (maximum initial rate) and k_{cat} = $1.65 \times 10^{2} h^{-1}$ (Turnover frequency) were obtained. Turnover frequency values (k_{cat}) were obtained by dividing the V_{max} values by the concentration of the BMG metallogel. The observed k_{cat} is 165 h^{-1} which is in good agreement with the literature reported values [30,31]. From this comparison of catecholase activity among different dinuclear complexes of copper, one can infer that our newly synthesized metallogel is an effective catalyst for oxidation of 3,5-DTBC to 3,5-DTBQ [34]. By comparison with different dinuclear and mononuclear copper model complexes that have been synthesized and used as catalysts for the oxidation of the widely used substrate 3,5-DTBC, we have successfully synthesized new bimetallic metallogels. The newly synthesized BMG acts as an efficient catalyst for the catalytic oxidation of 3,5-DTBC to 3,5-DTBQ. The catecholase mimetic catalytic activity of the current metallogel is comparable with the other copper-based catechol oxidase functional models with their kinetic parameters of DTBC oxidation listed in Table 2 [35,36]. When trying to correlate the catalytic parameters, the best models involve ligands with phenoxide bridges and aromatic imines, with the imine nitrogen acting as a donor atom. Despite the fact that the active site of the enzyme catechol oxidase contains a single hydroxo bridge, the ligand design with bis-phenoxo exhibits better results because of the improvement in efficiency despite the rigidity of the ligand binding the two copper(II) ions [37,38]. One benefit of the model systems over the original enzymes is that, in contrast to the natural enzymes, the model complexes may operate in organic solvents.

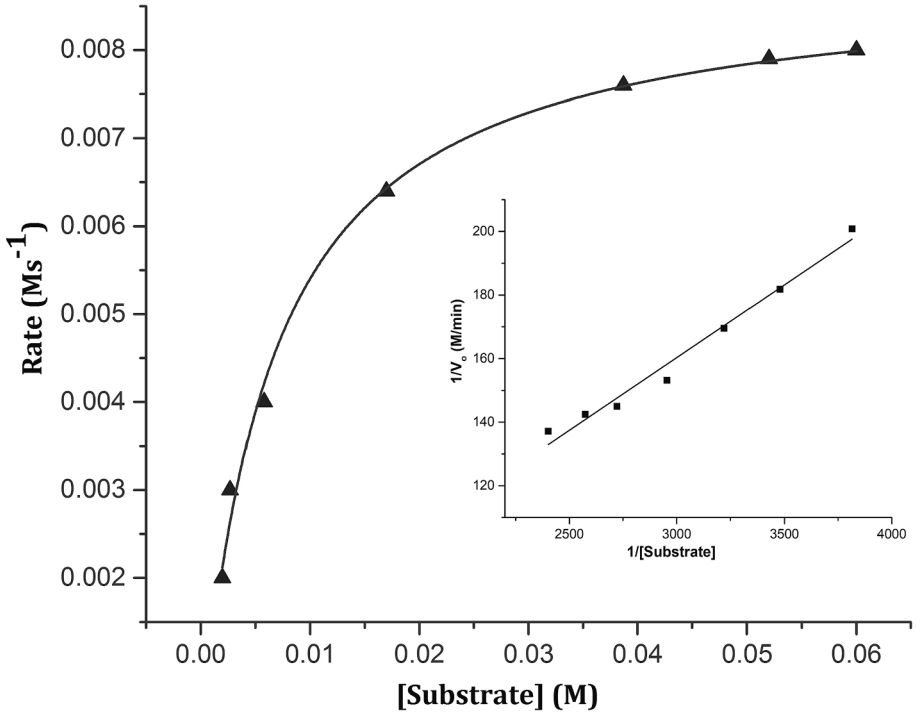

Fig. 5b. (B) Plot of rate vs concentration of BMG, inset represents Lineweaver-Burk plot.

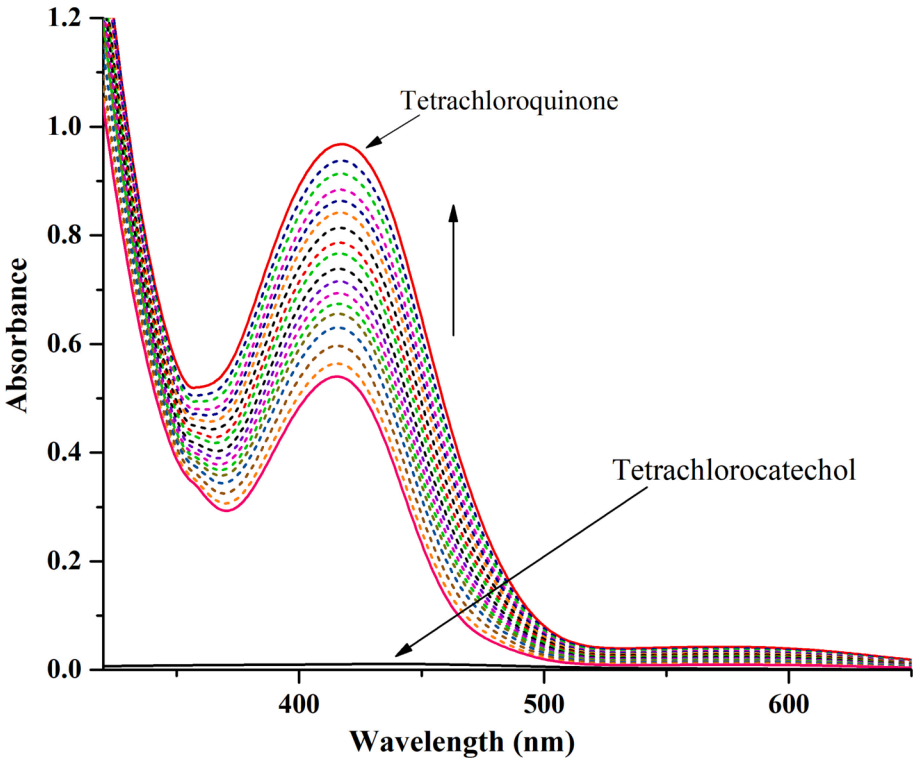

Fig. 6. Spectral changes observed for the absorbance at 415 nm as function of time (recorded at 2 min intervals).

Table 2
Comparison of K_{cat} value for oxidation of 3,5-DTBC to 3,5-DTBQ by various binuclear copper complexes.

Complex	Solvent	V_{max} ($Mmin^{-1}$)	K_M (M)	K_{cat} (h^{-1})
$[Cu_2(H_2$-bbppnol$)(\mu$-OAc$)(H_2O)_2]Cl_2{\cdot}2H_2O$ [ref.34]	Methanol	1.44×10^{-5}	7.9×10^{-4}	2.84×10^{1}
$[Cu_2($Hbtppnol$)(m$-OAc$)](ClO_4)_2$ [ref.34]	Methanol	1.44×10^{-5}	9.5×10^{-4}	2.81×10^{1}
$[Cu_2($P1-O-$)($OAc-$)](ClO_4)_2$ [ref. 34]	Methanol	4.02×10^{-5}	8.6×10^{-4}	1.08×10^{1}
$[Cu_2L^b_2(ClO_4)_2]$ [ref.35]	Methanol	1.56×10^{-4}	3.32×10^{-3}	9.36×10^{2}
$[Cu_2L^b_2(OH)]ClO_4$[ref.35]	Methanol	3.89×10^{-4}	4.60×10^{-3}	2.33×10^{2}
$[Cu_2Lc]$ [ref.36]	Methanol	6.74×10^{-3}	1.17×10^{-2}	7.22×10^{2}
$[Cu_2C_{41}H_{31}N_4O_6]PF_6$ Present work	DMSO	4.3×10^{-2}	1.98×10^{-3}	1.65×10^{2}

H_2btppnol = N-(2-hydroxybenzyl)-N,N0,N0-tris(2-pyridylmethyl)-1,3-diaminopropan-2-ol, P1-OH = 1,3-bis[bis(2-pyridylmethyl)amino] propanol, HL^b = 2-[[2-(diethylamino)-ethylamino]methyl]phenol.

We have proposed a plausible mechanism for generation of 3,5-DTBQ from 3,5-DTBC catalysed by BMG in the presence of air. Catalytic cycle is described in Scheme 2. On the basis of the above proposed mechanism, in the first step, the catecholate may then bind in a chelating fashion to one of the copper centers and simultaneously binds with substrate molecule. In the next step, molecular oxygen oxidizes to produce redox active phenoxyl radical species and such phenomenon indicates that phenoxo radical species are most probably generated during the catalytic cycle as compared with reported paper [38]. In the last step, Cu(II)-semiquinonate radical species reacts with molecular oxygen to generate 3,5-DTBQ along with H_2O as a by-product, and the catalytic cycle is completed with formation of BMG.

4. Conclusions

In conclusion, we report the synthesis of new bimetallic copper metallogel when copper acetate reacts with benzoic acid and bipyridine in aqueous DMF medium. The morphology of BMG has been explained with the help of scanning electron microscopy. The rheological investigation helps to examine and confirmed the gel nature of the material. Single X-ray diffraction studies verified the existence of pi-pi stacking, non-covalent interactions, and other short molecule interactions necessary for the formation of metallogel. In this work, we also report that BMG metallogel can act as an efficient catalyst for oxidation of 3,5-DTBC to 3,5-DTBQ and TCC to TCQ. The kinetic parameters have been derived by fitting the reaction profile in the Michaelis-Menten model and Lineweaver-Burk plot.

5. Author statement

The ideas were conceived by Dr. Sunshine Dominic Kurbah and prepared the manuscript. Dr. Ndege Simisi Clovis helps in collecting and visualization of data and Editing.

CRediT authorship contribution statement

Sunshine Dominic Kurbah: Writing – original draft, Visualization, Validation, Supervision, Software, Resources, Methodology, Investigation, Data curation, Conceptualization. **Ndege Simisi Clovis:** Writing – review & editing, Validation, Software, Formal analysis.

Declaration of competing interest

The authors declare that they have no known competing financial interests or personal relationships that could have appeared to influence the work reported in this paper.

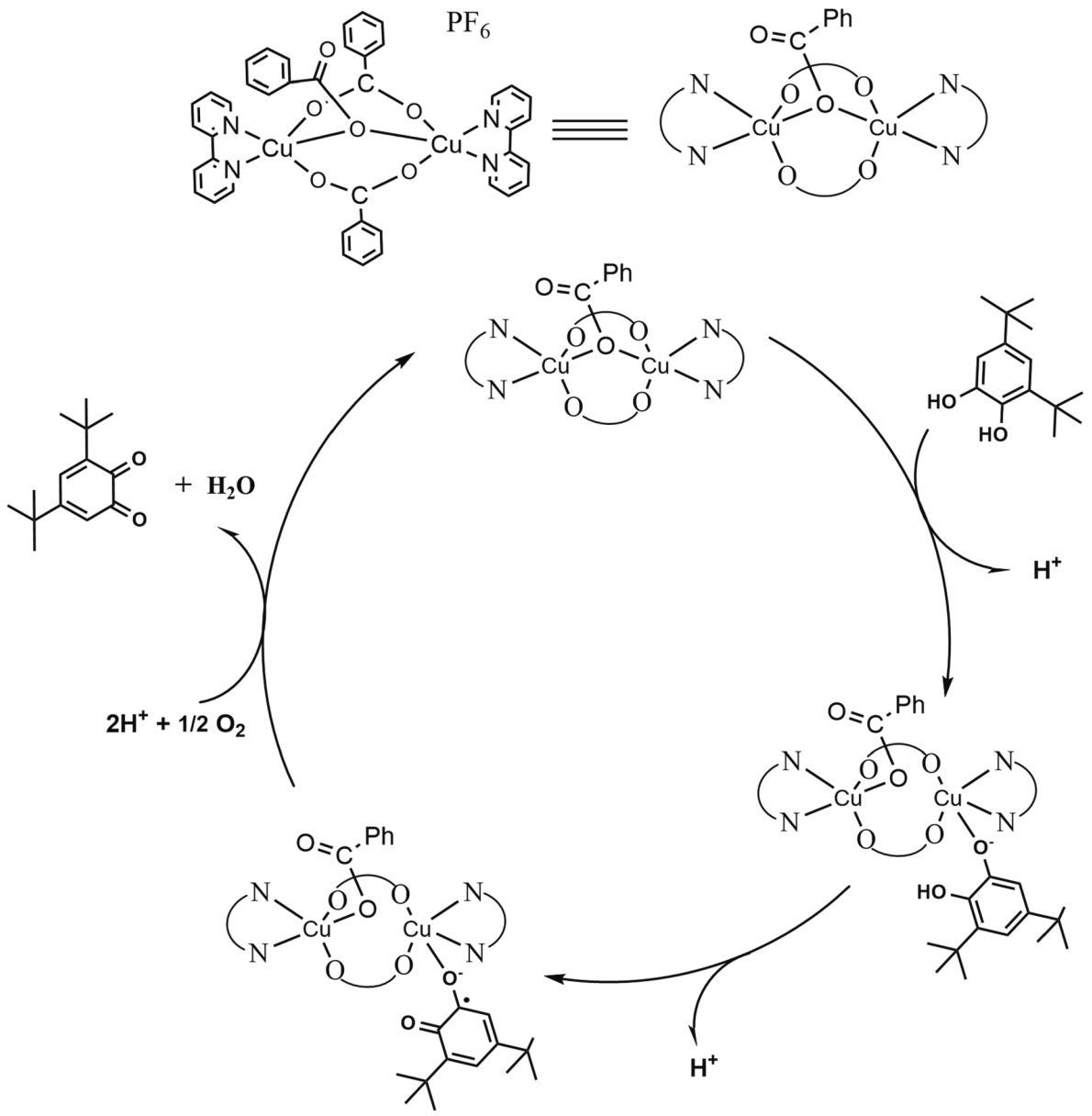

Scheme 2. A plausible mechanistic route for catechol oxidation catalyzed by BMG in presence of air.

Data availability

Data will be made available on request.

Acknowledgment

We would like to thank the Head, SAIF NEHU, for SEM analysis. IIT Bombay for X-ray crystallographic studies.

Appendix A. Supplementary data

Supplementary data to this article can be found online at https://doi.org/10.1016/j.ica.2024.122000.

References

[1] J. Zhuang, M.R. Gordon, J. Ventura, L. Li, S. Thayumanavan, Multi-stimuli responsive macromolecules and their assemblies, Chem. Soc. Rev. 42 (2013) 7421–7435.
[2] S.S. Babu, V.K. Praveen, A. Ajayaghosh, Functional π-G gelators and their applications, Chem. Rev. 114 (2014) 1973–11212.
[3] K. Sarkar, P. Dastidar, Rational approach towards designing metallogels from an urea-functionalized pyridyl dicarboxylate: anti-inflammatory, anticancer, and drug delivery, Chem. Asian J. 14 (2019) 194–1120.
[4] X. Du, J. Zhou, J. Shi, B. Xu, Supramolecular hydrogelators and hydrogels: from soft matter to molecular biomaterials, Chem. Rev. 115 (2015) 13165–13307.
[5] P. Biswas, S. Ganguly, P. Dastidar, Stimuli-responsive metallogels for synthesizing Ag nanoparticles and sensing hazardous gases, Chem. Eur. J. 13 (2018) 1941–1949.
[6] S.D. Kurbah, R.A. Lal, Bioinspired catalysis and bromoperoxidase like activity of a multistimuli-responsive supramolecular metallogel: supramolecular assembly triggered by pipi stacking and hydrogen bonding interactions, New J. Chem. 44 (2020) 5410–5418.
[7] A.Y.Y. Tam, V.W.W. Yam, Recent advances in metallogels, Chem. Soc. Rev. 42 (2013) 1540.
[8] S. Dhibar, A. Dey, S. Majumdar, D. Ghosh, A. Mandal, P.P. Ray, B. Dey, A supramolecular CD(II)-metallogel: an efficient semiconductive electronic device, Dalton Trans. 47 (2018) 17412–17420.
[9] A.A. Puranik, P.S. Salunke, N.D. Kulkarni, Supramolecular birefringent metallogels formed by trinuclear Copper(II) complexes with myo-inositol and bipyridyl ligands, New J. Chem. 43 (2019) 14720–14727.
[10] H. Hosseini-Monfared, C. Nather, H. Winkler, C. Janiak, Highly selective and "green'' alcohol oxidations in water using aqueous 10% H_2O_2 and iron-benzenetricarboxylate metal-organic gel, Inorg. Chim. Acta. 391 (2012) 75–82.

[11] S. Dhibar, A. Dey, D. Ghosh, S. Majumdar, A. Dey, P.P. Ray, B. Dey, Triethylenetetramine-based semiconducting FE(III) metallogel: effective catalyst for aryl-S coupling, ACS Omega. 5 (2020) 2680–2689.
[12] Y. Cui, B. Chen, G. Qian, Lanthanide metal-organic frameworks for luminescent sensing and light-emitting applications, Coord. Chem. Rev. 273 (2014) 76–86.
[13] O. Roubeau, A. Colin, V. Schmitt, R. Clerac, Thermoreversible gels as magneto-optical switches, Angew. Chem. Int. Ed. 43 (2004) 3283–3286.
[14] S. Sarkar, S. Dutta, P. Bairi, T. Pal, Redox-responsive copper (I) metallogel: a metal-organic hybrid sorbent for reductive removal of chromium (VI) from aqueous solution, Langmuir. 30 (2014) 7833–7841.
[15] A.R. Hirst, B. Escuder, J.F. Miravet, D.K. Smith, High-tech applications of self-assembling supramolecular nanostructured gel-phase materials: from regenerative medicine to electronic devices, Angew. Chem. Int. Ed. 47 (2008) 8002–8018.
[16] X.Q. Wang, W. Wang, G.Q. Yin, Cross-linked supramolecular polymer metallogels constructed via a self-sorting strategy and their multiple stimulus-response behaviors, Chem. Commun. 51 (2015) 16813–16816.
[17] S.C. Zacharias, G. Ramon, S.A. Bourne, Supramolecular metallogels constructed from carboxylate gelators, Soft Matter. 14 (2018) 4505–4519.
[18] W. Fang, Y. Zhang, J. Wu, C. Liu, H. Zhu, T. Tu, Recent advances in supramolecular gels and catalysis, Chem. Asian J. 13 (2018) 712–729.
[19] E. Saha, J. Mitra, Multistimuli-responsive self-healable and moldable Nickel(II)-based gels for reversible gas adsorption and palladium sequestration via gel-to-gel transformation, ACS Appl. Mater. Interfaces. 11 (2019) 10718–10728.
[20] S. Datta, S. Bhattacharya, Multifarious facets of sugar-derived molecular gels: molecular features, mechanisms of self-assembly and emerging applications, Chem. Soc. Rev. 44 (2015) 5596–5637.
[21] Y.X. Ye, W.L. Liu, B.H. Ye, A highly efficient and recyclable PD(II) metallogel catalyst: a new scaffold for Suzuki-Miyaura coupling, Cat. Com. 89 (2017) 100–105.
[22] H. Su, S. Zhu, M. Qu, R. Liu, G. Song, H. Zhu, 1,3,5-Triazine-based PT(II) metallogel material: synthesis, photophysical properties, and optical power-limiting performance, J Phys. Chem. C. 123 (2019) 15685–15692.
[23] T. Klabunde, C. Eicken, J.C. Sacchettini, B. Krebs, Crystal structure of a plant catechol oxidase containing a dicopper center, Nat. Struct. Biol. 5 (1998) 1084–1090.
[24] C. Gerdemann, C. Eicken, B. Krebs, The crystal structure of catechol oxidase: new insight into the function of Type-3 copper proteins, Acc. Chem. Res. 35 (2002) 183–191.
[25] C. Eicken, F. Zippel, K.B. Karentzopoulos, B. Krebs, Biochemical and spectroscopic characterization of catechol oxidase from sweet potatoes (Ipomoea batatas) containing a type-3 dicopper center, FEBS. Lett. 436 (1998) 293–299.
[26] K.S. Banu, T. Chattopadhyay, A. Banerjee, S. Bhattacharya, E. Zangrando, D. Das, Catechol oxidase activity of dinuclear Copper(II) complexes of Robson type macrocyclic ligands: syntheses, X-ray crystal structure, spectroscopic characterization of the adducts and kinetic studies, J. Mol. Cat. A: Chem. 310 (1–2) (2009) 34–41.
[27] S. Reja, A. Kejriwal, R.K. Das, Copper based biomimetic catalysts of catechol oxidase: an overview on recent trends, Catal. Ind. 15 (1) (2023) 108–124.
[28] K.S. Banu, T. Chattopadhyay, A. Banerjee, S. Bhattacharya, E. Suresh, M. Nethaji, E. Zangrando, D. Das, Catechol oxidase activity of a series of new dinuclear COPPER(II) complexes with 3,5-DTBC and TCC as substrates: syntheses, X-ray crystal structures, spectroscopic characterization of the adducts and kinetic studies, Inorg. Chem. 47 (16) (2008) 7083–7093.
[29] M.A. Chrisman, M.J. Goldcamp, A.N. Rhodes, J. Riffle, Exploring michaelis-menten kinetics and the inhibition of catalysis in a synthetic mimic of catechol oxidase: an experiment for the inorganic chemistry or biochemistry laboratory, J. Chem. Educ. 100 (2) (2023) 893–899.
[30] N. Malviya, C. Sonkar, B.K. Kundu, S. Mukhopadhyay, Discotic organic gelators in ion sensing, metallogel formation and bioinspired catalysis, Langmuir 34 (38) (2018) 11575–11585.
[31] A. Jana, N.A. Alcalde, E. Ruiz, S. Mohanta, Structures, magnetochemistry, spectroscopy, theoretical study, and catechol oxidase activity of dinuclear and dimer-of dinuclear mixed-valence Mn^{III} Mn^{II} complexes derived from a macrocyclic ligand, Inorg. Chem. 52 (2013) 7732–7746.
[32] G.M. Sheldrick, A short history of SHELX, Acta Crystallogr. Sect. a: Found. Crystallogr. 64 (2008) 112–122.
[33] G.M. Sheldrick, Crystal structure refinement with SHELXL, Acta Crystallogr. C: Struct Chem. Commun. 71 (2015) 3–8.
[34] A. Neves, L.M. Rossi, A.J. Bortoluzzi, B. Szpoganicz, C. Wiezbicki, E. Schwingel, W. Haase, S. Ostrovsky, Catecholase activity of a series of dicopper (II) complexes with variable cu-OH (phenol) moieties, Inorg. Chem. 41 (2002) 1788–1794.
[35] A. Biswas, L.K. Das, M.G.B. Drew, C. Diaz, A. Ghosh, Insertion of a hydroxido bridge into a diphenoxido dinuclear Copper(II) complex: drastic change of the magnetic property from strong antiferromagnetic to ferromagnetic and enhancement in the catecholase activity, Inorg. Chem. 51 (2012) 10111–10121.
[36] B. Mandal, M.C. Majee, T. Rakshit, S. Banerjee, P. Mitra, D. Mandal, Synthesis, structure, DFT study and catechol oxidase activity of Cu (II) complex with sterically constrained phenol based ligand, J. Mol. Struct. 1193 (2019) 265–273.
[37] Y. Hitomi, A. Ando, H. Matsui, T. Ito, T. Tanaka, S. Ogo, T. Funabiki, Aerobic catechol oxidation catalyzed by a bis (μ-oxo)dimanganese (III, III) complex via a manganese (II/III) semiquinonate complexes, Inorg. Chem. 44 (2005) 3473–3478.
[38] S.K. Dey, A. Mukherjee, Catechol oxidase and phenoxazinone synthase: biomimetic functional models and mechanistic studies, Coord. Chem. Rev. 310 (2016) 80–115.